Available online at www.sciencedirect.com
ScienceDirect
Bioresource Technology 99 (2008) 986–997
BIORESOURCE TECHNOLOGY

Non-isothermal thermogravimetric analysis of oil-palm solid wastes

P. Luangkiattikhun [a], C. Tangsathitkulchai [a,*], M. Tangsathitkulchai [b]

[a] School of Chemical Engineering, Suranaree University of Technology, Nakhon Ratchasima 30000, Thailand
[b] School of Chemistry, Suranaree University of Technology, Nakhon Ratchasima 30000, Thailand

Received 30 June 2006; received in revised form 7 March 2007; accepted 7 March 2007
Available online 23 April 2007

Abstract

Thermal decomposition of oil-palm solid wastes, including oil-palm shell, fibre and kernel, was studied by thermogravimetric analysis (TGA). Effect of heating rate and sample particle size on the behaviour of thermogram and kinetic parameters were investigated. The one-step global model, two-step consecutive model and two-parallel reactions model were used to simulate the pyrolysis process of the three materials studied. The one-step global model was able to describe the fractional weight loss upon pyrolysis of oil-palm kernel reasonably well but gave a large deviation for oil-palm shell and fibre. The two-step consecutive model could improve the fitting for oil-palm shell and fibre, but it cannot account for the inflection characteristic of the thermogram. Prediction by the two-parallel reactions model gave the best fitting with the experimental data of all oil-palm wastes under all pyrolysis conditions investigated. This proposed model was also tested with other biomass materials and proved to be satisfactory.

Keywords: Pyrolysis; Oil-palm solid wastes; TGA; DTG; Kinetic parameters

1. Introduction

The oil-palm (*Elaeis guineensis* Jacq.) was originally planted in West Africa, where local people have used it to make foodstuffs, medicines and wine. At the present time, oil-palm exists in a wild, semi-wild and cultivated state in the three land areas of equatorial tropics: Africa, South-East Asia and America (Hartley, 1988). Today large scales of oil-palm plantations are mostly for the production of palm oil, which is extracted from the flesh part of the palm fruit (mesocarp), and kernel oil, which is obtained from the innermost nut.

Oil-palm solid wastes (including shell, fibre and its kernel) are cheap and abandoned materials produced during palm oil milling process. For every ton of oil-palm fruit bunch being fed to the palm-oil refining process, about 0.07 tons of palm shell, 0.103 tons of palm fibre and 0.012 tons of kernel are produced as the solid wastes (Pansamut et al., 2003). Presently, approximately 154.2 and 5.1 megatons of oil-palm fresh fruit are processed annually worldwide and in Thailand, respectively (Centre of Agricultural Information, 2004). This means that more than 0.36 megatons of palm shell, 0.53 megatons of fibre, and 0.06 megatons are produced each year in Thailand. About 80% of these solid wastes are used as boiler fuel in many industries and 20% are abandoned (Pansamut et al., 2003). However, these renewable materials can be alternatively used for producing valuable chemical products (e.g., fuel, and chemical feedstock) by applying the thermochemical conversion processes, including pyrolysis, liquefaction and gasification as well as by supercritical fluid extraction methods (Yaman, 2004).

Among thermochemical conversion processes, pyrolysis is a viable process for biomass upgrading by cracking polymeric structure of lignocellulosic materials and converting it into a volatile fraction consisting of gases, vapours and tar components and a carbon rich solid residue (char) fractions. The volatile fraction can be used as a fuel or as a chemical feedstock. For the remaining solid fraction, it can be used in several applications, for example, in the production of activated carbon or used directly as a solid fuel.

* Corresponding author. Tel.: +66 44 22 4263; fax: +66 44 22 4609.
E-mail address: chaiyot@sut.ac.th (C. Tangsathitkulchai).

0960-8524/$ - see front matter © 2007 Elsevier Ltd. All rights reserved.
doi:10.1016/j.biortech.2007.03.001

The knowledge and understanding on pyrolysis kinetics of biomass are important for proper design of a pyrolysis reactor which plays an important role in large-scale pyrolysis process. The pyrolysis kinetics can be studied by several methods but the most popular and simplest technique is the thermogravimetric analysis (TGA) (Haines, 1995). In this method, the change of a sample mass is monitored against time or temperature in the absence of oxygen at a specific heating rate. Important parameters that determine the quality and yield of pyrolysis products are heating rate, final temperature, holding time at the final temperature and the nature and physical properties of raw materials (Bansal et al., 1988).

The decomposition of carbonaceous matter during pyrolysis is very complicated and depends also on heat transfer by convection, conduction and radiation. Some simplified numerical models were proposed in literatures to predict the decomposition rate and final yield of char and volatile matter. Wichman and Atreya (1987) applied a one-step global model for predicting the devolatilization rate of pyrolysis process. They assumed that the carbonaceous sample is decomposed in one-step to produce the volatile substance and solid char. Bellais et al. (2003) developed a shrinkage model for the pyrolysis of large wood particles. The shrinkage was considered in three different ways: uniform shrinkage, shrinking shell and shrinking cylinders. All shrinkage models show good agreements with the experimental results for mass loss versus time at high temperature range (higher than 600 °C) but fail to simulate correctly at low temperatures. Thurner and Mann (1981) proposed the three-parallel reactions model to describe thermal decomposition of a carbonaceous material into gas, tar and char. Chan et al. (1985) developed a pyrolysis model with three primary reactions (parallel reaction) and one secondary reaction (tar decomposing into gas and char).

For oil palm-shell, Guo and Lua (2001) have applied the one-step global model and the two-step consecutive model for simulating the pyrolysis process. The one-step global model showed faster pyrolysis conversion than the actual experimental values, especially, at the high temperature region. The two-step consecutive model agreed quite well with the experimental data. However, this model consists of a set of three ODEs which has no analytical solution. Its accuracy depends on the size of time step and numerical techniques used in the calculation.

In this work, the kinetics of pyrolysis reaction of palm shell, fibre and kernel were studied by using the thermogravimetric analysis (TGA) technique (Haines, 1995). Effects of raw material particle size and heating rate on the shape of thermograms were investigated. The two-parallel reactions model which leads to only one analytical solution was applied to simulate the pyrolysis process of oil-palm shell, fibre and kernel. The validity of this proposed model was also tested with other different carbonaceous materials, including coconut shell, bagasse, longan seed and cassava pulp residue.

2. Model description

The two-parallel reactions model used in this work was originally proposed by Font et al. (1991). They used this model for describing the pyrolysis scheme of almond shell by assuming that the almond shell consists of two independent fractions which decompose at different rates and temperatures. Therefore, there are two main competing reactions which occur simultaneously. In addition, the first-order kinetics for both competing reactions was assumed. In the present work, however, the first-order kinetic scheme was also assumed for the first fraction, but the order of reaction was set as a free parameter for the second fraction, with a purpose to increase model flexibility.

Basic assumptions of the two-parallel reactions model are that the reaction is kinetically controlled and there are no secondary reactions among the released gaseous products. It is further assumed that the raw material consists of two homogeneous matters, M_1 and M_2 and each component decomposes simultaneously at different rate and temperature, producing volatile matters and solid char. The overall reaction and the two individual parallel reactions are expressed by Eqs. (1) and (2), respectively.

$$\text{Raw material} \xrightarrow{k_T} \text{Volatile 1} + \text{Volatile 2} + \text{char} \tag{1}$$

$$M_1 \xrightarrow{k_1} \text{Volatile 1} + \text{char} \tag{2-a}$$

$$M_2 \xrightarrow{k_2} \text{Volatile 2} + \text{char} \tag{2-b}$$

where k_1 and k_2 represent the rate constants of each reaction. The residual weight fraction of char components are defined as follows:

$$\alpha = \frac{M - m_f}{1 - m_f}; \quad \alpha_1 = \frac{M_1 - m_{f1}}{1 - m_f}; \quad \alpha_2 = \frac{M_2 - m_{f2}}{1 - m_f} \tag{3}$$

where m_f is the final yield of char which is estimated from the final constant weight of TG curve. m_{f1} and m_{f2} are the final yields of the first and second components presented in the raw material, respectively. M, M_1 and M_2 are mass fractions of total char, solid char of components 1 and 2 present at time t, respectively, with

$$M = M_1 + M_2 \tag{4-a}$$

$$m_f = m_{f1} + m_{f2} \tag{4-b}$$

The rate of decomposition reaction in Eqs. (2-a) and (2-b) are assumed to follow:

$$\frac{d\alpha_1}{dt} = -A_1 \exp\left(\frac{-E_1}{RT}\right)\alpha_1 \tag{5-a}$$

$$\frac{d\alpha_2}{dt} = -A_2 \exp\left(\frac{-E_2}{RT}\right)\alpha_2^n \tag{5-b}$$

where A is the frequency or pre-exponential factor, E is the activation energy, R is the universal gas constant, T is the absolute temperature, n is the order of decomposition

reaction for component 2 and t is the time. For a constant heating rate, β, we can write

$$\frac{dT}{dt} = \beta \tag{6}$$

Dividing Eq. (5) by Eq. (6), the rate of decomposition reactions can be expressed as a function of temperature as follows:

$$\frac{d\alpha_1}{dT} = -\frac{A_1}{\beta}\exp\left(\frac{-E_1}{RT}\right)\alpha_1 \tag{7-a}$$

$$\frac{d\alpha_2}{dT} = -\frac{A_2}{\beta}\exp\left(\frac{-E_2}{RT}\right)\alpha_2^n \tag{7-b}$$

Rearranging Eq. (7) and integrating to obtain

$$\int_a^{\alpha_1}\frac{d\alpha_1}{\alpha_1} = -\frac{A_1}{\beta}\int_0^T \exp\left(\frac{-E_1}{RT}\right)dT \tag{8-a}$$

$$\int_b^{\alpha_2}\frac{d\alpha_2}{\alpha_2^n} = -\frac{A_2}{\beta}\int_0^T \exp\left(\frac{-E_2}{RT}\right)dT \tag{8-b}$$

where a and b are initial values of α_1 and α_2, respectively, and they indicate the initial weight fractions of component 1 and 2 in the starting raw material. They are assumed constant and depend only on the characteristics of the raw material. The relationship between a and b is expressed as

$$a + b = 1 \tag{9}$$

The exponential term on the right-hand side of Eq. (8) can be expressed in an asymptotic series and by neglecting the higher order terms, the integration yields (Guo and Lua, 2001)

$$\frac{A_i}{\beta}\int_0^T \exp\left(\frac{-E_i}{RT}\right)dT = \frac{A_i RT^2}{\beta E_i}\left[1 - \frac{2RT}{E_i}\right]\exp\left(\frac{-E_i}{RT}\right) \tag{10}$$

Substitution of Eq. (10) into Eq. (8), the expressions of α_1 and α_2 can be derived as follows:

$$\alpha_1 = \exp\left[\frac{-A_1RT^2}{\beta E_1}\left(1 - \frac{2RT}{E_1}\right)\exp\left(\frac{-E_1}{RT}\right) + \ln(a)\right] \tag{11-a}$$

$$\alpha_2 = \left[\frac{(n-1)A_2RT^2}{\beta E_2}\left(1 - \frac{2RT}{E_2}\right)\exp\left(\frac{-E_2}{RT}\right) + b^{(1-n)}\right]^{\frac{1}{1-n}} \tag{11-b}$$

The total of remaining mass at any temperature is the sum of each residual fraction. That is,

$$\alpha = \alpha_1 + \alpha_2 = \exp\left[\frac{-A_1RT^2}{\beta E_1}\left(1 - \frac{2RT}{E_1}\right)\exp\left(\frac{-E_1}{RT}\right) + \ln(a)\right] + \left[\frac{(n-1)A_2RT^2}{\beta E_2}\left(1 - \frac{2RT}{E_2}\right)\exp\left(\frac{-E_2}{RT}\right) + b^{(1-n)}\right]^{\frac{1}{1-n}} \tag{12}$$

Eq. (12) was used to fit the experimental TG data and the six kinetic parameters (a, A_1, E_1, A_2, E_2 and n) were determined through model fitting by minimizing the sum of square of relative error (SSRE), defined as

$$\mathrm{SSRE} = \sum\left(\frac{\alpha_{exp} - \alpha_{model}}{\alpha_{exp}}\right)^2 \tag{13}$$

where α_{exp} and α_{model} are the experimental and simulated residual fraction, respectively.

3. Experimental

The kinetic study of pyrolysis reaction was carried out by following the mass of a sample as a function of temperature using a thermogravimetric analyzer (TGA 7, Perkin Elmer). Oil-palm solid wastes, including shell, fibre and kernel were supplied by Golden Palm Industry in Chon Buri Province, Thailand. The received materials were washed and dried at 110 °C for 24 h. Then, they were crushed and sieved to obtain average particle sizes of 0.36, 0.51, 0.73, 1.1 and 1.4 mm for oil-palm shell, less than 1.0 mm and 0.25 mm for fibre and kernel, respectively. Table 1 shows the proximate and ultimate analyses of the three biomass samples studied in this work. The solid densities of raw materials were measured by using a helium pycnometer.

A sample of about 10 mg was placed into the TGA equipment and heated from room temperature to 700 °C at various heating rates from 5 to 40 °C/min. Ultra high purity grade of nitrogen (99.9995% purity supplied by TIG, Thailand) at a constant flow rate of 100 cm^3/min was used as a purge gas to provide an inert atmosphere around the sample during devolatilization and to carry away the pyrolyzed products from the reaction zones. Variation of sample mass with respect to temperature change (TG data) and its first derivative (DTG data) were continuously collected. The derived TG data was fitted with the one-step global model, two-step consecutive model and two-parallel reactions model to test the predictive capability of the models by using optimization function in

Table 1
Proximate and ultimate analysis of the oil-palm shell, fibre and kernel

Sample	Ultimate analysis (% w/w)					Proximate analysis			Solid density (g/cm^3)
	C	H	N	S	O	Volatile	Fix-C	Ash	
Palm shell	47.6	5.38	0.66	0.04	41.38	72.7	23.6	3.6	1.42
Palm fibre	46.64	5.66	1.73	0.10	39.46	73.7	12.6	6.6	0.75
Palm kernel	41.47	5.77	3.00	0.03	43.49	80.3	10.3	3.2	1.39

MATLAB program. The kinetic parameters were then followed from the model fitting results.

4. Results and discussion

Thermal decomposition of oil-palm shell, fibre and kernel was studied at four different heating rates of 5, 10, 20 and 40 °C/min and five average particle sizes (only for oil-palm shell) of 0.36, 0.51, 0.72, 1.10 and 1.40 mm to investigate their effect on the behaviour of thermogram and kinetic parameters of the pyrolysis process. The experimental data of all three materials were fitted with the simplest kinetic scheme, the one-step global model, and also with the more complex kinetic models, the two-step consecutive model of Guo and Lua (2001) and two-parallel reactions model proposed in this work. Also presented in this section are the pyrolysis data and results of model fitting of other potential biomasses, including coconut shell, bagasse, longan seed and cassava pulp residue.

4.1. Analysis of the thermograms

The thermogravimetric (TG) data and its first derivative (DTG data) of oil-palm shell, fibre and kernel pyrolyzed at the heating rate of 20 °C/min are plotted against the temperature in the same graph in order to show their kinetic scheme (see Fig. 1). Results show that the pyrolysis of oil-palm solid wastes commenced at the temperature above 250 °C for palm shell and above 200 °C for palm fibre and kernel. For the pyrolysis of oil-palm shell and fibre, there are two distinct peaks of DTG curves which indicate that there should be at least two main groups of reaction occurring during the decomposition process. It is noted that the two maximum of decomposition rates occur at about 300 °C and 375 °C for both oil-palm shell and fibre, respectively.

It is known that the major components of lignocellulosic biomass are hemicellulose, cellulose and lignin (Antal, 1983). The main thermal decomposition of lignocellulosic materials generally occurs over the temperature range of 200–400 °C. Lignin is the first component to decompose at a low temperature and low rate and continues on until approximately 900 °C. Hemicellulose is a light fraction component which also decomposes at the low temperature region between 160 and 360 °C. Cellulose is the last component to decompose at the high temperature range of 240–390 °C (Vamvuka et al., 2003). The existing of two major peaks observed in DTG curves may be qualitatively explained as follows. The first peak could be generated by the decomposition of hemicellulose and some of the lignin. The second peak should correspond to the decomposition of cellulose and the remaining lignin (Font et al., 1991; Tsamba et al., 2006). At the temperatures above 400 °C, the final decomposition involves the aromatization process of lignin fraction leading to very low weight loss (Fisher et al., 2002). Based on this reasoning, it might be logical

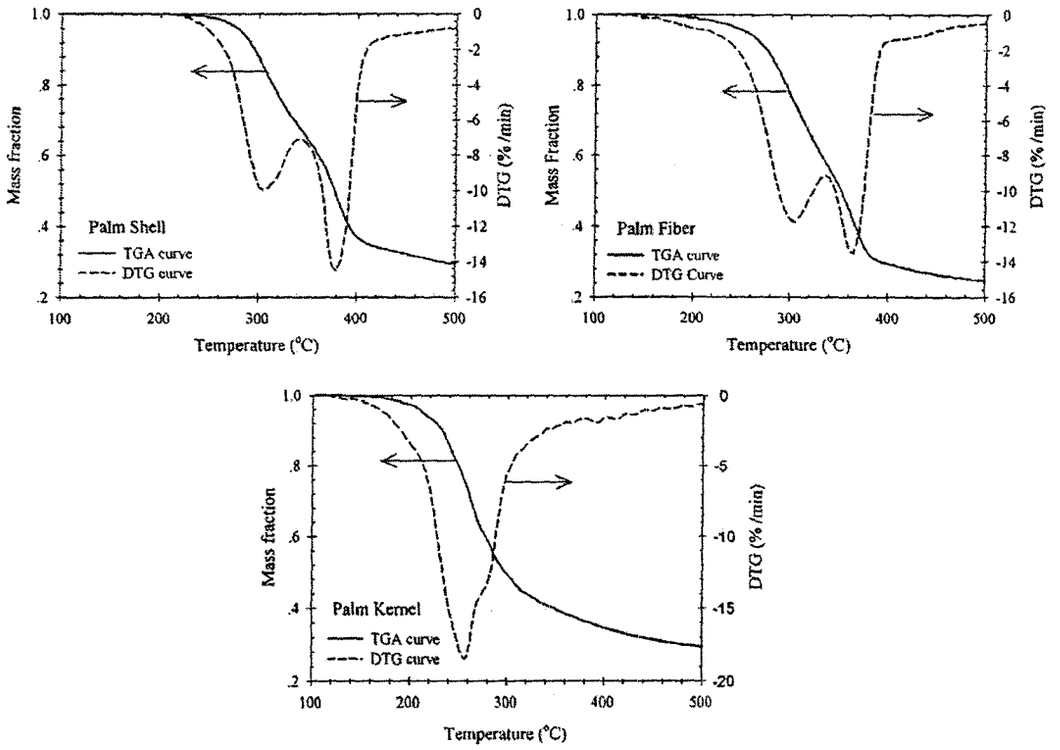

Fig. 1. TG and DTG data of oil-palm shell, fibre and kernel pyrolyzed at heating rate of 20 °C/min.

to test the experimental kinetic data of palm shell and fibre using the two-parallel reactions and two-step consecutive model.

For oil-palm kernel (see Fig. 1), there is only one maximum rate of decomposition observed at about 250 °C with a small shoulder located at the higher temperature side on the DTG curve. This indicates that there is at least one major reaction scheme occurring during the pyrolysis process for this type of material. The maximum peak of DTG curve is probably contributed by the decomposition of the lighter fraction (i.e. hemicellulose) and the small shoulder corresponds to the decomposition of the heavier component (i.e. cellulose). It is observed that the rate of decomposition of the light component for the case of oil-palm kernel is greater than the rate of decomposition of the heavy component, while for oil-palm shell and fibre, the rate of decomposition of the heavy component is dominated. The one peak of DTG data with small shoulder was also found for the pyrolysis of olive-kernel as reported by Vamvuka et al. (2003). With the existence of only one peak of DTG data, it is expected that the experimental data of oil-palm kernel could be described by the one-step global model.

It is known that particle size is an important parameter that can affect the pyrolysis behaviour (Haykiri-Acma, 2006; Jayaweera et al., 1989; Kok et al., 1998; Larsen et al., 2006). An increasing in particle size can establish the temperature gradient, causing increased heat transfer resistance inside the pyrolyzed particles, which in turn can cause an increase in the final solid yield and a decrease of volatile matter released during the pyrolysis process. The residual weight fractions of oil-palm shell determined during pyrolysis process (TG data) are shown in Fig. 2, for various particle sizes at the heating rate of 20 °C/min. As observed, the particle size has no significant effect on the thermogram of oil-palm shell at the initial stage of pyrolysis (temperature lower than 320 °C), after that the residual mass of sample and the final yield of char increase with increasing of particle size at the same pyrolysis temperature. However, the decomposition of solid appears to start and end at approximately the same temperature range for all particle size studied here. Also shown in Fig. 2 is the first derivative of mass change with respect to temperature (DTG data) for various particle sizes at the heating rate of 20 °C/min. The plots show that the first and second peaks of DTG curve occur at approximately the same temperature independent of particle sizes (see also in Table 2).

Figs. 3–5 show respectively the thermograms of oil-palm shell, fibre and kernel pyrolyzed at various heating rates. It is observed that as the heating rate is increased the thermograms of palm shell and fibre shifted systematically to higher temperature region but slightly shifted for the case of palm kernel. These results indicate that palm shell and fibre decomposed at a higher temperature when a higher heating rate was applied. The shift of thermograms to higher temperature region is probably due to the effect of heat transfer which causes the temperature lag between the surrounding and inside of the particle. However, there is no measurable effect of heating rate on the final yield of char for all three materials. The same results can be

Table 2
First and second maximum rate of decomposition and corresponding temperatures of oil-palm solid wastes

Sample	Heating rate (°C/min)	Size (mm)	$T_{1,max}$	1st maximum rate (%/min)	$T_{2,max}$	2nd maximum rate (%/min)
Shell	20	0.36	305	−9.95	380	−14.49
		0.51	305	−10.06	375	−13.30
		0.73	305	−9.77	380	−14.08
		1.10	300	−10.19	380	−13.46
		1.40	300	−10.04	380	−13.38
Shell	5	0.36	280	−2.50	355	−4.20
	10		295	−5.02	365	−7.80
	20		305	−9.95	380	−14.49
	40		320	−21.14	390	−26.13
Fibre	5	<1.00	280	−3.06	340	−4.14
	10		295	−5.76	350	−7.44
	20		305	−11.76	365	−13.55
	40		310	−27.06	370	−27.34
Kernel	5	<0.15	250	−4.53	–	–
	10		245	−9.20	–	–
	20		255	−18.41	–	–
	40		255	−43.42	–	–

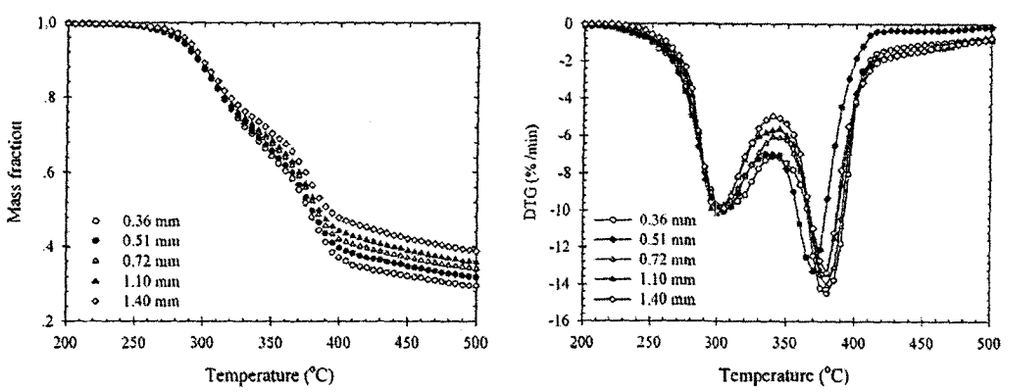

Fig. 2. TG and DTG data of oil-palm shell pyrolyzed at heating rate 20 °C/min for various particle sizes.

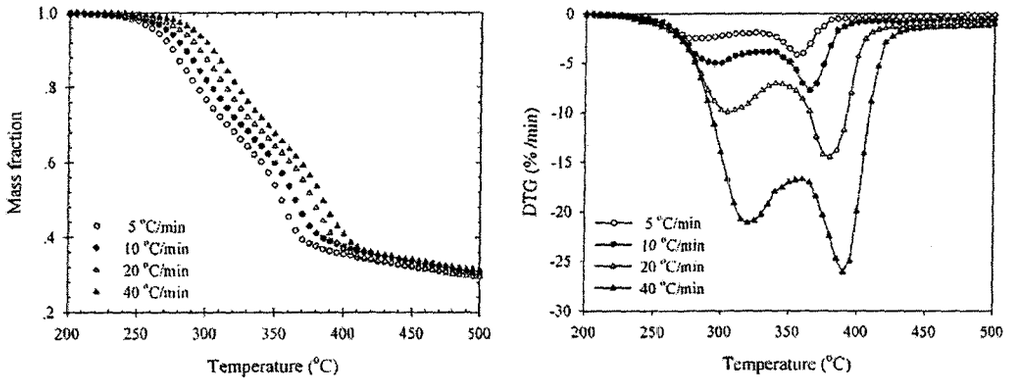

Fig. 3. TG and DTG data of oil-palm shell pyrolyzed at particle size 0.36 mm for various heating rates.

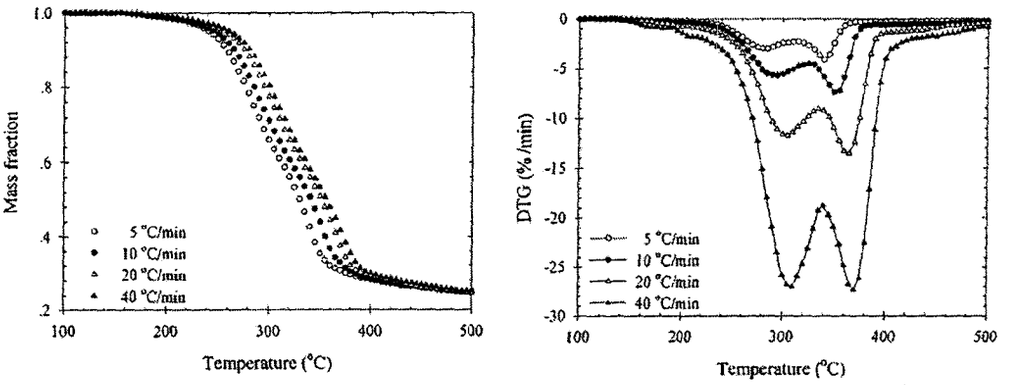

Fig. 4. TG and DTG data of oil-palm fibre pyrolyzed at different heating rates.

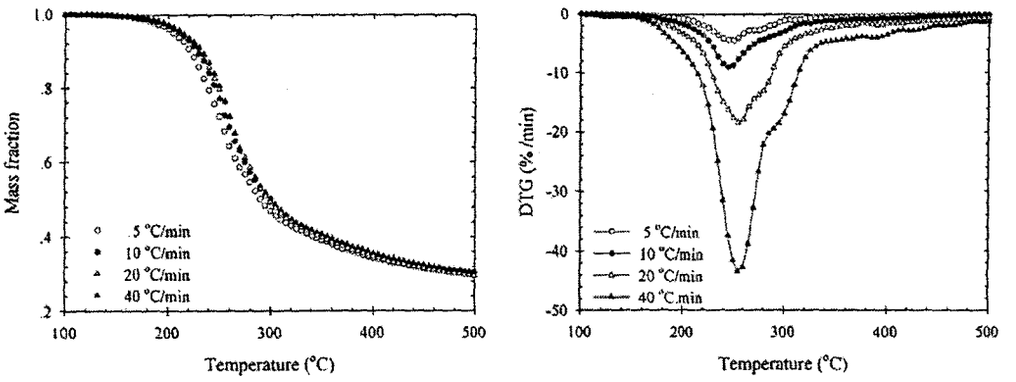

Fig. 5. TG and DTG data of oil-palm kernel pyrolyzed at different heating rates.

observed in the pyrolysis of almond shell and olive stone as reported by Caballero et al. (1997).

Also shown in Figs. 3–5 are the DTG data of oil-palm shell, fibre and kernel pyrolyzed at various heating rates. The heating rate affects significantly on the maximum decomposition rate, with maximum decomposition rate tending to increase and occur at higher temperatures when pyrolyzed at higher heating rates. The first and second maximum rates of decomposition and the corresponding temperatures are summarized in Table 2.

4.2. One-step global model

The one-step global model is the simplest kinetic model for describing the decomposition process of carbonaceous materials. This model assumes that the rate of decomposi-

tion can be expressed by one kinetic scheme. Mathematically,

$$\frac{d\alpha}{dT} = \frac{A}{\beta} e^{-E/RT}(1-\alpha)^n \quad (14)$$

here, the residual weight fraction, α, is defined in terms of the change in the mass of sample as

$$\alpha = \frac{w_0 - w}{w_0 - w_f} \quad (15)$$

where w_0, w and w_f are the initial, actual and final mass of the sample, respectively.

Fig. 6 shows the comparison between experimental data and model fitting with the one-step global model for oil-palm shell, fibre and kernel at different heating rates. The agreement between experimental data and the one-step global model prediction is considered acceptable, however, the model cannot account for the inflection of thermograms for all heating rates. The maximum deviations for the pyrolysis of oil-palm shell and fibre lie in the range of 10–15%. For oil-palm kernel, the model agrees well with the experimental data with less than 4% of the maximum deviation for all heating rates.

The kinetic parameters, the order of reaction (n), activation energy (E) and frequency factor (A) determined from the model fitting are summarized in Table 3. The frequency factor and activation energy of oil-palm shell and kernel appear to increase with increasing of heating rate, while a decrease is observed for the case of oil-palm fibre. The frequency factor and activation energy indicate how fast and easy for the pyrolysis reaction to proceed. The higher frequency factor and lower activation energy, the faster and easier would be for the pyrolysis reaction to occur. The order of reaction decreases with increasing of heating rate for oil-palm shell and fibre, but it increases for the case of oil-palm kernel. The order of reaction for all three materials is in the range of 2.5–4.0.

Table 3
Kinetic parameters of one-step global model for pyrolysis of oil-palm shell, fibre and kernel

Samples	Heating rate (°C/min)	A (s^{-1})	E (kJ/mol)	n	Max. error (%)
Palm shell	5	7.93×10^6	106.1	2.84	11.90
	10	2.05×10^7	109.1	2.65	9.22
	20	4.84×10^7	110.4	2.52	10.71
	40	5.27×10^7	111.0	2.54	9.51
Palm fibre	5	1.52×10^{10}	136.0	3.35	10.83
	10	1.96×10^9	125.9	3.32	14.69
	20	1.50×10^9	124.1	2.95	11.84
	40	1.00×10^9	123.3	2.87	10.93
Palm kernel	5	4.57×10^{13}	156.1	3.37	2.99
	10	1.24×10^{14}	159.5	3.41	2.98
	20	1.31×10^{15}	167.5	3.52	3.56
	40	2.34×10^{16}	176.4	3.85	3.87

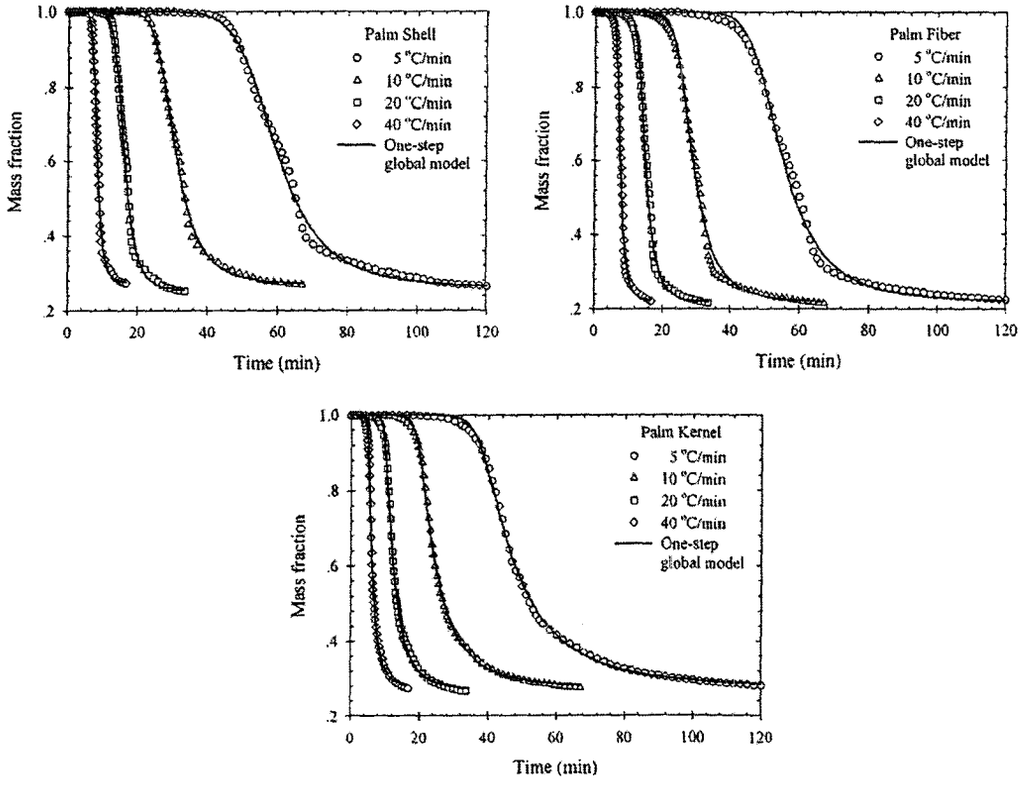

Fig. 6. TG data and one-step global model fitting of oil-palm shell, fibre and kernel.

Available online at www.sciencedirect.com
ScienceDirect
Bioresource Technology 99 (2008) 986–997
BIORESOURCE TECHNOLOGY

Non-isothermal thermogravimetric analysis of oil-palm solid wastes

P. Luangkiattikhun [a], C. Tangsathitkulchai [a,*], M. Tangsathitkulchai [b]

[a] School of Chemical Engineering, Suranaree University of Technology, Nakhon Ratchasima 30000, Thailand
[b] School of Chemistry, Suranaree University of Technology, Nakhon Ratchasima 30000, Thailand

Received 30 June 2006; received in revised form 7 March 2007; accepted 7 March 2007
Available online 23 April 2007

Abstract

Thermal decomposition of oil-palm solid wastes, including oil-palm shell, fibre and kernel, was studied by thermogravimetric analysis (TGA). Effect of heating rate and sample particle size on the behaviour of thermogram and kinetic parameters were investigated. The one-step global model, two-step consecutive model and two-parallel reactions model were used to simulate the pyrolysis process of the three materials studied. The one-step global model was able to describe the fractional weight loss upon pyrolysis of oil-palm kernel reasonably well but gave a large deviation for oil-palm shell and fibre. The two-step consecutive model could improve the fitting for oil-palm shell and fibre, but it cannot account for the inflection characteristic of the thermogram. Prediction by the two-parallel reactions model gave the best fitting with the experimental data of all oil-palm wastes under all pyrolysis conditions investigated. This proposed model was also tested with other biomass materials and proved to be satisfactory.

Keywords: Pyrolysis; Oil-palm solid wastes; TGA; DTG; Kinetic parameters

1. Introduction

The oil-palm (*Elaeis guineensis* Jacq.) was originally planted in West Africa, where local people have used it to make foodstuffs, medicines and wine. At the present time, oil-palm exists in a wild, semi-wild and cultivated state in the three land areas of equatorial tropics: Africa, South-East Asia and America (Hartley, 1988). Today large scales of oil-palm plantations are mostly for the production of palm oil, which is extracted from the flesh part of the palm fruit (mesocarp), and kernel oil, which is obtained from the innermost nut.

Oil-palm solid wastes (including shell, fibre and its kernel) are cheap and abandoned materials produced during palm oil milling process. For every ton of oil-palm fruit bunch being fed to the palm-oil refining process, about 0.07 tons of palm shell, 0.103 tons of palm fibre and 0.012 tons of kernel are produced as the solid wastes (Pansamut et al., 2003). Presently, approximately 154.2 and 5.1 megatons of oil-palm fresh fruit are processed annually worldwide and in Thailand, respectively (Centre of Agricultural Information, 2004). This means that more than 0.36 megatons of palm shell, 0.53 megatons of fibre, and 0.06 megatons are produced each year in Thailand. About 80% of these solid wastes are used as boiler fuel in many industries and 20% are abandoned (Pansamut et al., 2003). However, these renewable materials can be alternatively used for producing valuable chemical products (e.g., fuel, and chemical feedstock) by applying the thermochemical conversion processes, including pyrolysis, liquefaction and gasification as well as by supercritical fluid extraction methods (Yaman, 2004).

Among thermochemical conversion processes, pyrolysis is a viable process for biomass upgrading by cracking polymeric structure of lignocellulosic materials and converting it into a volatile fraction consisting of gases, vapours and tar components and a carbon rich solid residue (char) fractions. The volatile fraction can be used as a fuel or as a chemical feedstock. For the remaining solid fraction, it can be used in several applications, for example, in the production of activated carbon or used directly as a solid fuel.

* Corresponding author. Tel.: +66 44 22 4263; fax: +66 44 22 4609.
E-mail address: chaiyot@sut.ac.th (C. Tangsathitkulchai).

0960-8524/$ - see front matter © 2007 Elsevier Ltd. All rights reserved.
doi:10.1016/j.biortech.2007.03.001

The knowledge and understanding on pyrolysis kinetics of biomass are important for proper design of a pyrolysis reactor which plays an important role in large-scale pyrolysis process. The pyrolysis kinetics can be studied by several methods but the most popular and simplest technique is the thermogravimetric analysis (TGA) (Haines, 1995). In this method, the change of a sample mass is monitored against time or temperature in the absence of oxygen at a specific heating rate. Important parameters that determine the quality and yield of pyrolysis products are heating rate, final temperature, holding time at the final temperature and the nature and physical properties of raw materials (Bansal et al., 1988).

The decomposition of carbonaceous matter during pyrolysis is very complicated and depends also on heat transfer by convection, conduction and radiation. Some simplified numerical models were proposed in literatures to predict the decomposition rate and final yield of char and volatile matter. Wichman and Atreya (1987) applied a one-step global model for predicting the devolatilization rate of pyrolysis process. They assumed that the carbonaceous sample is decomposed in one-step to produce the volatile substance and solid char. Bellais et al. (2003) developed a shrinkage model for the pyrolysis of large wood particles. The shrinkage was considered in three different ways: uniform shrinkage, shrinking shell and shrinking cylinders. All shrinkage models show good agreements with the experimental results for mass loss versus time at high temperature range (higher than 600 °C) but fail to simulate correctly at low temperatures. Thurner and Mann (1981) proposed the three-parallel reactions model to describe thermal decomposition of a carbonaceous material into gas, tar and char. Chan et al. (1985) developed a pyrolysis model with three primary reactions (parallel reaction) and one secondary reaction (tar decomposing into gas and char).

For oil palm-shell, Guo and Lua (2001) have applied the one-step global model and the two-step consecutive model for simulating the pyrolysis process. The one-step global model showed faster pyrolysis conversion than the actual experimental values, especially, at the high temperature region. The two-step consecutive model agreed quite well with the experimental data. However, this model consists of a set of three ODEs which has no analytical solution. Its accuracy depends on the size of time step and numerical techniques used in the calculation.

In this work, the kinetics of pyrolysis reaction of palm shell, fibre and kernel were studied by using the thermogravimetric analysis (TGA) technique (Haines, 1995). Effects of raw material particle size and heating rate on the shape of thermograms were investigated. The two-parallel reactions model which leads to only one analytical solution was applied to simulate the pyrolysis process of oil-palm shell, fibre and kernel. The validity of this proposed model was also tested with other different carbonaceous materials, including coconut shell, bagasse, longan seed and cassava pulp residue.

2. Model description

The two-parallel reactions model used in this work was originally proposed by Font et al. (1991). They used this model for describing the pyrolysis scheme of almond shell by assuming that the almond shell consists of two independent fractions which decompose at different rates and temperatures. Therefore, there are two main competing reactions which occur simultaneously. In addition, the first-order kinetics for both competing reactions was assumed. In the present work, however, the first-order kinetic scheme was also assumed for the first fraction, but the order of reaction was set as a free parameter for the second fraction, with a purpose to increase model flexibility.

Basic assumptions of the two-parallel reactions model are that the reaction is kinetically controlled and there are no secondary reactions among the released gaseous products. It is further assumed that the raw material consists of two homogeneous matters, M_1 and M_2 and each component decomposes simultaneously at different rate and temperature, producing volatile matters and solid char. The overall reaction and the two individual parallel reactions are expressed by Eqs. (1) and (2), respectively.

$$\text{Raw material} \xrightarrow{k_T} \text{Volatile 1} + \text{Volatile 2} + \text{char} \tag{1}$$

$$M_1 \xrightarrow{k_1} \text{Volatile 1} + \text{char} \tag{2-a}$$

$$M_2 \xrightarrow{k_2} \text{Volatile 2} + \text{char} \tag{2-b}$$

where k_1 and k_2 represent the rate constants of each reaction. The residual weight fraction of char components are defined as follows:

$$\alpha = \frac{M - m_f}{1 - m_f}; \quad \alpha_1 = \frac{M_1 - m_{f1}}{1 - m_f}; \quad \alpha_2 = \frac{M_2 - m_{f2}}{1 - m_f} \tag{3}$$

where m_f is the final yield of char which is estimated from the final constant weight of TG curve. m_{f1} and m_{f2} are the final yields of the first and second components presented in the raw material, respectively. M, M_1 and M_2 are mass fractions of total char, solid char of components 1 and 2 present at time t, respectively, with

$$M = M_1 + M_2 \tag{4-a}$$

$$m_f = m_{f1} + m_{f2} \tag{4-b}$$

The rate of decomposition reaction in Eqs. (2-a) and (2-b) are assumed to follow:

$$\frac{d\alpha_1}{dt} = -A_1 \exp\left(\frac{-E_1}{RT}\right)\alpha_1 \tag{5-a}$$

$$\frac{d\alpha_2}{dt} = -A_2 \exp\left(\frac{-E_2}{RT}\right)\alpha_2^n \tag{5-b}$$

where A is the frequency or pre-exponential factor, E is the activation energy, R is the universal gas constant, T is the absolute temperature, n is the order of decomposition

reaction for component 2 and t is the time. For a constant heating rate, β, we can write

$$\frac{dT}{dt} = \beta \tag{6}$$

Dividing Eq. (5) by Eq. (6), the rate of decomposition reactions can be expressed as a function of temperature as follows:

$$\frac{d\alpha_1}{dT} = -\frac{A_1}{\beta}\exp\left(\frac{-E_1}{RT}\right)\alpha_1 \tag{7-a}$$

$$\frac{d\alpha_2}{dT} = -\frac{A_2}{\beta}\exp\left(\frac{-E_2}{RT}\right)\alpha_2^n \tag{7-b}$$

Rearranging Eq. (7) and integrating to obtain

$$\int_a^{\alpha_1}\frac{d\alpha_1}{\alpha_1} = -\frac{A_1}{\beta}\int_0^T \exp\left(\frac{-E_1}{RT}\right)dT \tag{8-a}$$

$$\int_b^{\alpha_2}\frac{d\alpha_2}{\alpha_2^n} = -\frac{A_2}{\beta}\int_0^T \exp\left(\frac{-E_2}{RT}\right)dT \tag{8-b}$$

where a and b are initial values of α_1 and α_2, respectively, and they indicate the initial weight fractions of component 1 and 2 in the starting raw material. They are assumed constant and depend only on the characteristics of the raw material. The relationship between a and b is expressed as

$$a + b = 1 \tag{9}$$

The exponential term on the right-hand side of Eq. (8) can be expressed in an asymptotic series and by neglecting the higher order terms, the integration yields (Guo and Lua, 2001)

$$\frac{A_i}{\beta}\int_0^T \exp\left(\frac{-E_i}{RT}\right)dT = \frac{A_i RT^2}{\beta E_i}\left[1 - \frac{2RT}{E_i}\right]\exp\left(\frac{-E_i}{RT}\right) \tag{10}$$

Substitution of Eq. (10) into Eq. (8), the expressions of α_1 and α_2 can be derived as follows:

$$\alpha_1 = \exp\left[\frac{-A_1RT^2}{\beta E_1}\left(1 - \frac{2RT}{E_1}\right)\exp\left(\frac{-E_1}{RT}\right) + \ln(a)\right] \tag{11-a}$$

$$\alpha_2 = \left[\frac{(n-1)A_2RT^2}{\beta E_2}\left(1 - \frac{2RT}{E_2}\right)\exp\left(\frac{-E_2}{RT}\right) + b^{(1-n)}\right]^{\frac{1}{1-n}} \tag{11-b}$$

The total of remaining mass at any temperature is the sum of each residual fraction. That is,

$$\begin{aligned}\alpha &= \alpha_1 + \alpha_2 \\ &= \exp\left[\frac{-A_1RT^2}{\beta E_1}\left(1 - \frac{2RT}{E_1}\right)\exp\left(\frac{-E_1}{RT}\right) + \ln(a)\right] \\ &\quad + \left[\frac{(n-1)A_2RT^2}{\beta E_2}\left(1 - \frac{2RT}{E_2}\right)\exp\left(\frac{-E_2}{RT}\right) + b^{(1-n)}\right]^{\frac{1}{1-n}}\end{aligned} \tag{12}$$

Eq. (12) was used to fit the experimental TG data and the six kinetic parameters (a, A_1, E_1, A_2, E_2 and n) were determined through model fitting by minimizing the sum of square of relative error (SSRE), defined as

$$\mathrm{SSRE} = \sum\left(\frac{\alpha_{exp} - \alpha_{model}}{\alpha_{exp}}\right)^2 \tag{13}$$

where α_{exp} and α_{model} are the experimental and simulated residual fraction, respectively.

3. Experimental

The kinetic study of pyrolysis reaction was carried out by following the mass of a sample as a function of temperature using a thermogravimetric analyzer (TGA 7, Perkin Elmer). Oil-palm solid wastes, including shell, fibre and kernel were supplied by Golden Palm Industry in Chon Buri Province, Thailand. The received materials were washed and dried at 110 °C for 24 h. Then, they were crushed and sieved to obtain average particle sizes of 0.36, 0.51, 0.73, 1.1 and 1.4 mm for oil-palm shell, less than 1.0 mm and 0.25 mm for fibre and kernel, respectively. Table 1 shows the proximate and ultimate analyses of the three biomass samples studied in this work. The solid densities of raw materials were measured by using a helium pycnometer.

A sample of about 10 mg was placed into the TGA equipment and heated from room temperature to 700 °C at various heating rates from 5 to 40 °C/min. Ultra high purity grade of nitrogen (99.9995% purity supplied by TIG, Thailand) at a constant flow rate of 100 cm^3/min was used as a purge gas to provide an inert atmosphere around the sample during devolatilization and to carry away the pyrolyzed products from the reaction zones. Variation of sample mass with respect to temperature change (TG data) and its first derivative (DTG data) were continuously collected. The derived TG data was fitted with the one-step global model, two-step consecutive model and two-parallel reactions model to test the predictive capability of the models by using optimization function in

Table 1
Proximate and ultimate analysis of the oil-palm shell, fibre and kernel

Sample	Ultimate analysis (% w/w)					Proximate analysis			Solid density (g/cm^3)
	C	H	N	S	O	Volatile	Fix-C	Ash	
Palm shell	47.6	5.38	0.66	0.04	41.38	72.7	23.6	3.6	1.42
Palm fibre	46.64	5.66	1.73	0.10	39.46	73.7	12.6	6.6	0.75
Palm kernel	41.47	5.77	3.00	0.03	43.49	80.3	10.3	3.2	1.39

MATLAB program. The kinetic parameters were then followed from the model fitting results.

4. Results and discussion

Thermal decomposition of oil-palm shell, fibre and kernel was studied at four different heating rates of 5, 10, 20 and 40 °C/min and five average particle sizes (only for oil-palm shell) of 0.36, 0.51, 0.72, 1.10 and 1.40 mm to investigate their effect on the behaviour of thermogram and kinetic parameters of the pyrolysis process. The experimental data of all three materials were fitted with the simplest kinetic scheme, the one-step global model, and also with the more complex kinetic models, the two-step consecutive model of Guo and Lua (2001) and two-parallel reactions model proposed in this work. Also presented in this section are the pyrolysis data and results of model fitting of other potential biomasses, including coconut shell, bagasse, longan seed and cassava pulp residue.

4.1. Analysis of the thermograms

The thermogravimetric (TG) data and its first derivative (DTG data) of oil-palm shell, fibre and kernel pyrolyzed at the heating rate of 20 °C/min are plotted against the temperature in the same graph in order to show their kinetic scheme (see Fig. 1). Results show that the pyrolysis of oil-palm solid wastes commenced at the temperature above 250 °C for palm shell and above 200 °C for palm fibre and kernel. For the pyrolysis of oil-palm shell and fibre, there are two distinct peaks of DTG curves which indicate that there should be at least two main groups of reaction occurring during the decomposition process. It is noted that the two maximum of decomposition rates occur at about 300 °C and 375 °C for both oil-palm shell and fibre, respectively.

It is known that the major components of lignocellulosic biomass are hemicellulose, cellulose and lignin (Antal, 1983). The main thermal decomposition of lignocellulosic materials generally occurs over the temperature range of 200–400 °C. Lignin is the first component to decompose at a low temperature and low rate and continues on until approximately 900 °C. Hemicellulose is a light fraction component which also decomposes at the low temperature region between 160 and 360 °C. Cellulose is the last component to decompose at the high temperature range of 240–390 °C (Vamvuka et al., 2003). The existing of two major peaks observed in DTG curves may be qualitatively explained as follows. The first peak could be generated by the decomposition of hemicellulose and some of the lignin. The second peak should correspond to the decomposition of cellulose and the remaining lignin (Font et al., 1991; Tsamba et al., 2006). At the temperatures above 400 °C, the final decomposition involves the aromatization process of lignin fraction leading to very low weight loss (Fisher et al., 2002). Based on this reasoning, it might be logical

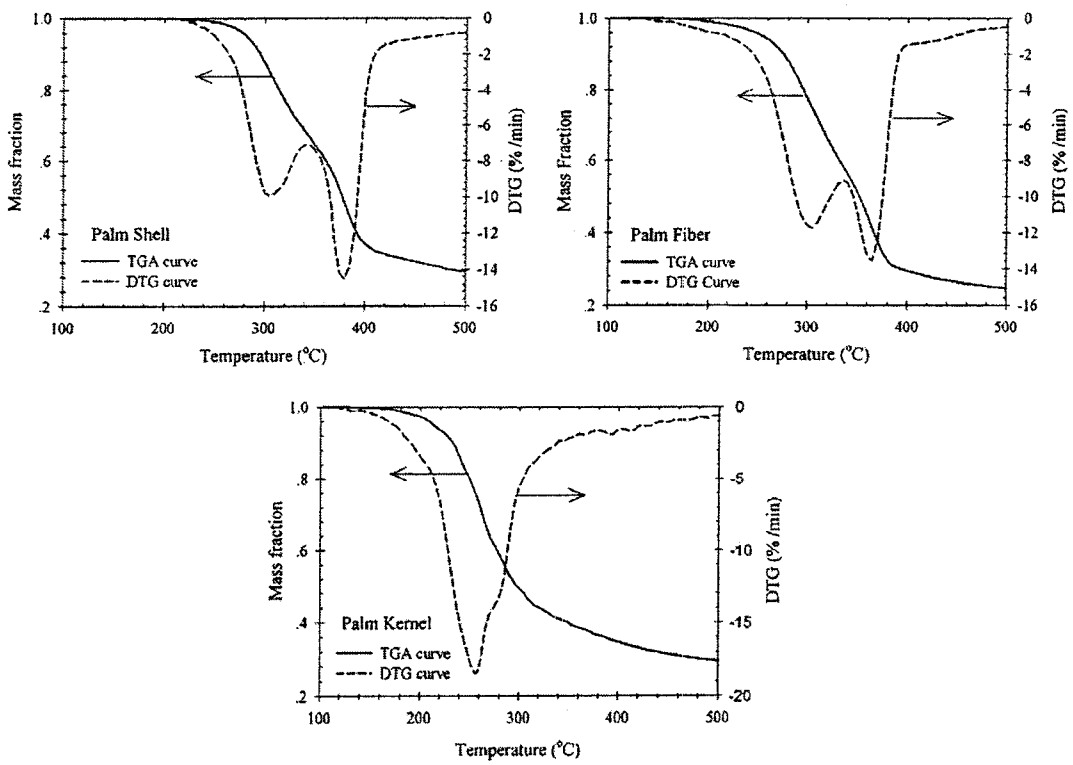

Fig. 1. TG and DTG data of oil-palm shell, fibre and kernel pyrolyzed at heating rate of 20 °C/min.

to test the experimental kinetic data of palm shell and fibre using the two-parallel reactions and two-step consecutive model.

For oil-palm kernel (see Fig. 1), there is only one maximum rate of decomposition observed at about 250 °C with a small shoulder located at the higher temperature side on the DTG curve. This indicates that there is at least one major reaction scheme occurring during the pyrolysis process for this type of material. The maximum peak of DTG curve is probably contributed by the decomposition of the lighter fraction (i.e. hemicellulose) and the small shoulder corresponds to the decomposition of the heavier component (i.e. cellulose). It is observed that the rate of decomposition of the light component for the case of oil-palm kernel is greater than the rate of decomposition of the heavy component, while for oil-palm shell and fibre, the rate of decomposition of the heavy component is dominated. The one peak of DTG data with small shoulder was also found for the pyrolysis of olive-kernel as reported by Vamvuka et al. (2003). With the existence of only one peak of DTG data, it is expected that the experimental data of oil-palm kernel could be described by the one-step global model.

It is known that particle size is an important parameter that can affect the pyrolysis behaviour (Haykiri-Acma, 2006; Jayaweera et al., 1989; Kok et al., 1998; Larsen et al., 2006). An increasing in particle size can establish the temperature gradient, causing increased heat transfer resistance inside the pyrolyzed particles, which in turn can cause an increase in the final solid yield and a decrease of volatile matter released during the pyrolysis process. The residual weight fractions of oil-palm shell determined during pyrolysis process (TG data) are shown in Fig. 2, for various particle sizes at the heating rate of 20 °C/min. As observed, the particle size has no significant effect on the thermogram of oil-palm shell at the initial stage of pyrolysis (temperature lower than 320 °C), after that the residual mass of sample and the final yield of char increase with increasing of particle size at the same pyrolysis temperature. However, the decomposition of solid appears to start and end at approximately the same temperature range for all particle size studied here. Also shown in Fig. 2 is the first derivative of mass change with respect to temperature (DTG data) for various particle sizes at the heating rate of 20 °C/min. The plots show that the first and second peaks of DTG curve occur at approximately the same temperature independent of particle sizes (see also in Table 2).

Figs. 3–5 show respectively the thermograms of oil-palm shell, fibre and kernel pyrolyzed at various heating rates. It is observed that as the heating rate is increased the thermograms of palm shell and fibre shifted systematically to higher temperature region but slightly shifted for the case of palm kernel. These results indicate that palm shell and fibre decomposed at a higher temperature when a higher heating rate was applied. The shift of thermograms to higher temperature region is probably due to the effect of heat transfer which causes the temperature lag between the surrounding and inside of the particle. However, there is no measurable effect of heating rate on the final yield of char for all three materials. The same results can be

Table 2
First and second maximum rate of decomposition and corresponding temperatures of oil-palm solid wastes

Sample	Heating rate (°C/min)	Size (mm)	$T_{1,max}$	1st maximum rate (%/min)	$T_{2,max}$	2nd maximum rate (%/min)
Shell	20	0.36	305	−9.95	380	−14.49
		0.51	305	−10.06	375	−13.30
		0.73	305	−9.77	380	−14.08
		1.10	300	−10.19	380	−13.46
		1.40	300	−10.04	380	−13.38
Shell	5	0.36	280	−2.50	355	−4.20
	10		295	−5.02	365	−7.80
	20		305	−9.95	380	−14.49
	40		320	−21.14	390	−26.13
Fibre	5	<1.00	280	−3.06	340	−4.14
	10		295	−5.76	350	−7.44
	20		305	−11.76	365	−13.55
	40		310	−27.06	370	−27.34
Kernel	5	<0.15	250	−4.53	–	–
	10		245	−9.20	–	–
	20		255	−18.41	–	–
	40		255	−43.42	–	–

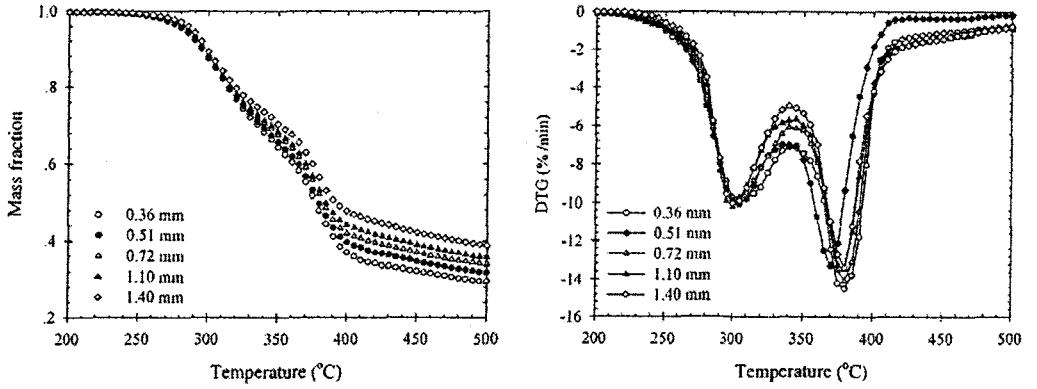

Fig. 2. TG and DTG data of oil-palm shell pyrolyzed at heating rate 20 °C/min for various particle sizes.

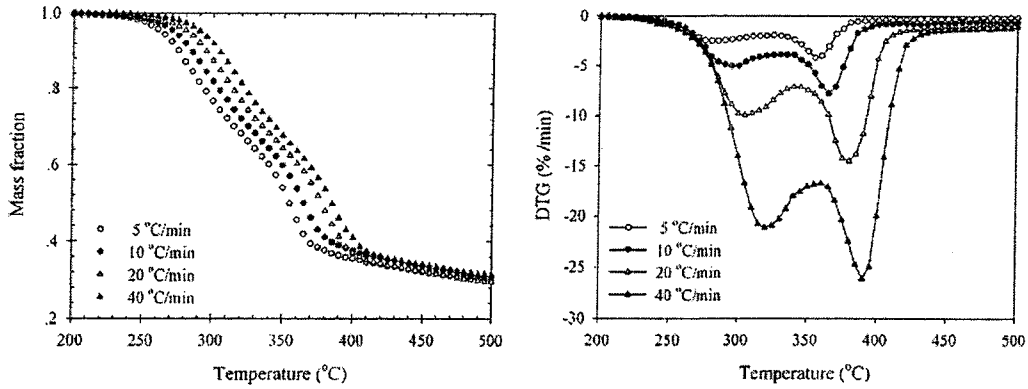

Fig. 3. TG and DTG data of oil-palm shell pyrolyzed at particle size 0.36 mm for various heating rates.

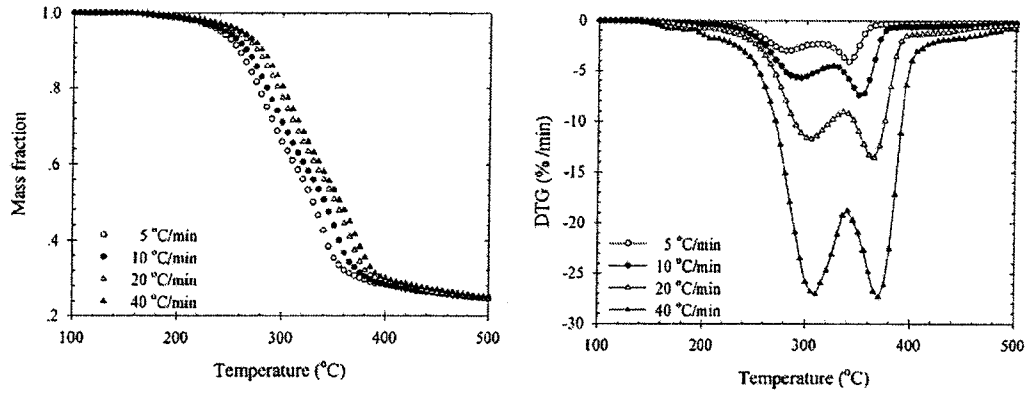

Fig. 4. TG and DTG data of oil-palm fibre pyrolyzed at different heating rates.

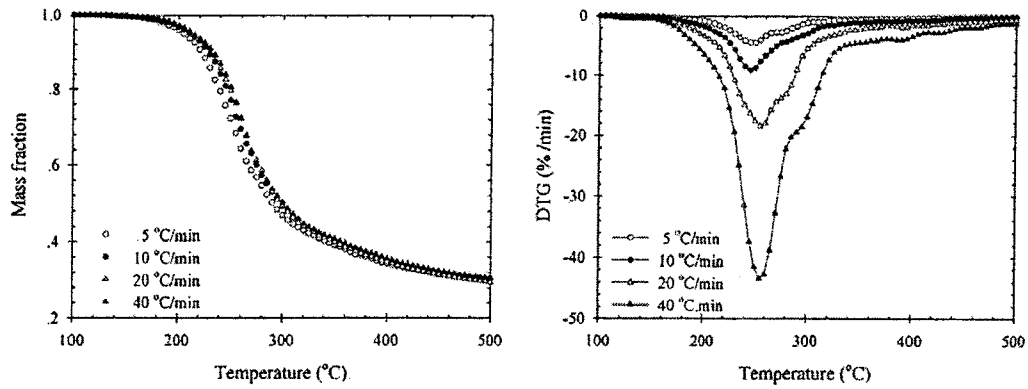

Fig. 5. TG and DTG data of oil-palm kernel pyrolyzed at different heating rates.

observed in the pyrolysis of almond shell and olive stone as reported by Caballero et al. (1997).

Also shown in Figs. 3–5 are the DTG data of oil-palm shell, fibre and kernel pyrolyzed at various heating rates. The heating rate affects significantly on the maximum decomposition rate, with maximum decomposition rate tending to increase and occur at higher temperatures when pyrolyzed at higher heating rates. The first and second maximum rates of decomposition and the corresponding temperatures are summarized in Table 2.

4.2. One-step global model

The one-step global model is the simplest kinetic model for describing the decomposition process of carbonaceous materials. This model assumes that the rate of decomposi-

tion can be expressed by one kinetic scheme. Mathematically,

$$\frac{d\alpha}{dT} = \frac{A}{\beta} e^{-E/RT}(1-\alpha)^n \quad (14)$$

here, the residual weight fraction, α, is defined in terms of the change in the mass of sample as

$$\alpha = \frac{w_0 - w}{w_0 - w_f} \quad (15)$$

where w_0, w and w_f are the initial, actual and final mass of the sample, respectively.

Fig. 6 shows the comparison between experimental data and model fitting with the one-step global model for oil-palm shell, fibre and kernel at different heating rates. The agreement between experimental data and the one-step global model prediction is considered acceptable, however, the model cannot account for the inflection of thermograms for all heating rates. The maximum deviations for the pyrolysis of oil-palm shell and fibre lie in the range of 10–15%. For oil-palm kernel, the model agrees well with the experimental data with less than 4% of the maximum deviation for all heating rates.

The kinetic parameters, the order of reaction (n), activation energy (E) and frequency factor (A) determined from the model fitting are summarized in Table 3. The frequency factor and activation energy of oil-palm shell and kernel appear to increase with increasing of heating rate, while a decrease is observed for the case of oil-palm fibre. The frequency factor and activation energy indicate how fast and easy for the pyrolysis reaction to proceed. The higher frequency factor and lower activation energy, the faster and easier would be for the pyrolysis reaction to occur. The order of reaction decreases with increasing of heating rate for oil-palm shell and fibre, but it increases for the case of oil-palm kernel. The order of reaction for all three materials is in the range of 2.5–4.0.

Table 3
Kinetic parameters of one-step global model for pyrolysis of oil-palm shell, fibre and kernel

Samples	Heating rate (°C/min)	A (s^{-1})	E (kJ/mol)	n	Max. error (%)
Palm shell	5	7.93×10^6	106.1	2.84	11.90
	10	2.05×10^7	109.1	2.65	9.22
	20	4.84×10^7	110.4	2.52	10.71
	40	5.27×10^7	111.0	2.54	9.51
Palm fibre	5	1.52×10^{10}	136.0	3.35	10.83
	10	1.96×10^9	125.9	3.32	14.69
	20	1.50×10^9	124.1	2.95	11.84
	40	1.00×10^9	123.3	2.87	10.93
Palm kernel	5	4.57×10^{13}	156.1	3.37	2.99
	10	1.24×10^{14}	159.5	3.41	2.98
	20	1.31×10^{15}	167.5	3.52	3.56
	40	2.34×10^{16}	176.4	3.85	3.87

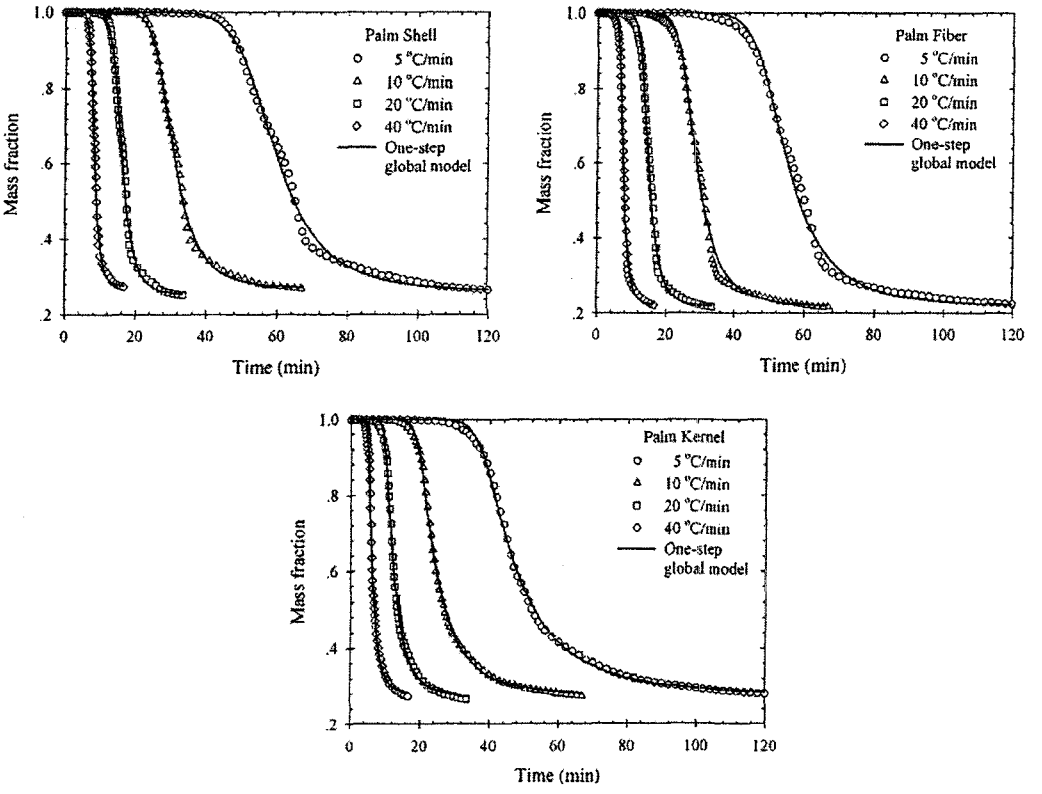

Fig. 6. TG data and one-step global model fitting of oil-palm shell, fibre and kernel.

Due to the two-peak characteristic of DTG data, the pyrolysis process of oil-palm shell and fibre should be best described by a model consisting of two-stage kinetic scheme. In this work, two simple kinetic models, which are the two-step consecutive model (Guo and Lua, 2001) and the two-parallel reactions model (Font et al., 1991), were explored.

4.3. Two-step consecutive model

The two-step consecutive model was used by Guo and Lua (2001) in studying the kinetics of pyrolysis reaction of oil-palm shell by using the thermogravimetric method. Basic assumptions of this model are that the reaction is a pure kinetic controlled process and there are no secondary reactions among the gaseous products.

The model was assumed to consist of two reaction steps (as shown in Eqs. (16) and (17)). The starting material first decomposes to produce the first group of volatile matters and the intermediate substance which further decompose to produce the final solid char and the second group of volatile matters. That is,

$$W \xrightarrow{k_1} x.I + \text{Volatile (1)} \tag{16}$$

$$I \xrightarrow{k_2} y.C + \text{Volatile (2)} \tag{17}$$

where W, I and C are the weight fraction of raw material, intermediate and solid char, respectively, and x and y are the stoichiometric coefficients of the reactions. The kinetic equation for decomposition of raw material and generation of the intermediate and final solid char can be described by the following expressions:

$$\frac{dW}{dT} = -\frac{A_1}{\beta} e^{-E_1/RT} W \tag{18}$$

$$\frac{dI}{dT} = -\frac{xA_1}{\beta} e^{-E_1/RT} W - \frac{A_2}{\beta} e^{-E_2/RT} I^n \tag{19}$$

$$\frac{dC}{dT} = \frac{yA_2}{\beta} e^{-E_2/RT} I^n \tag{20}$$

where n is the order of the second step of pyrolysis reaction. The relationship between x and y can be obtained from the mass balance which is written as the following:

$$x = \frac{m_f}{y} \tag{21}$$

where m_f is the final yield of char. The initial conditions for the above three ordinary differential equations are

$$W = 1, \quad I = C = 1 \text{ at } T = 0\,\text{K} \tag{22}$$

The residual weight fraction of sample at any temperature and time is equal to the summation of raw material, intermediate and char. We solve the above set of ordinary differential equations by using ODE solver in MATLAB program.

The two-step consecutive model was tested against the experimental data of oil-palm shell, fibre and kernel from

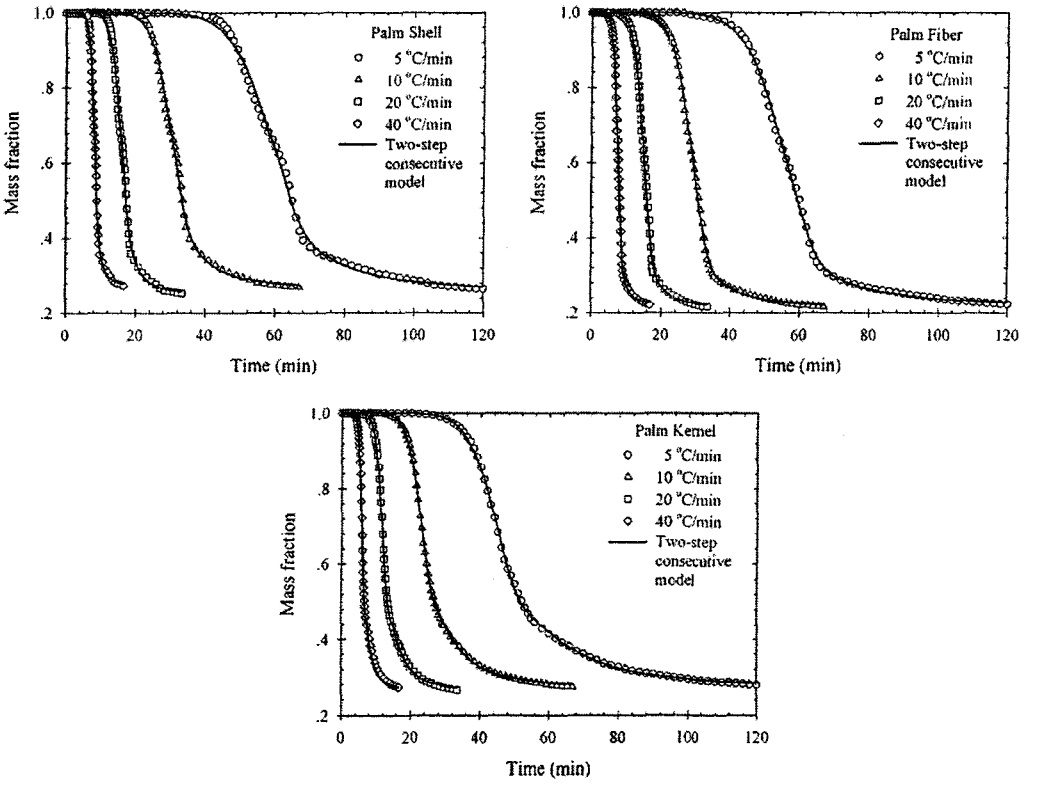

Fig. 7. TG data and two-step consecutive model fitting of oil-palm shell, fibre and kernel.

the present study and the results are shown in Fig. 7. The two-step consecutive model shows the improvement of model fitting for oil-palm shell and fibre over the one-step global model. The maximum deviation for oil-palm shell and fibre are in the range of 4–7%. However, the two-step consecutive model cannot fully account for the inflection of the thermograms, particularly at low heating rates. For oil-palm kernel, the two-step consecutive model also gives good agreement with the experimental data with the range of percentage error being the same order as that of the one-step global model. These results confirm that the one-step global model is sufficient to describe the pyrolysis process of oil-palm kernel which shows only one peak of DTG curve.

The kinetic parameters determined from the model fitting for the two-step consecutive model are listed in Table 4. The frequency factor of raw material (A_1) increases with increasing of heating rate for all three materials studied here. Although the activation energy of raw material (E_1) decrease with increasing of heating rate for all materials, but the overall rate constant still increase. This observation indicates that the raw material decomposes at a faster rate when the heating rate is increased. This trend of simulated results agrees with the experimental data of DTG curves (see Figs. 3–5) which show the increasing in decomposition rate for the first peak when heating rate is increased for all three materials. For the decomposition of intermediate to form solid char, the frequency factor (A_2) decreases when the heating rate is increased for the case of oil-palm shell and fibre, whereas they increase for the case of oil-palm kernel. For activation energy (E_2), it decreases with increasing of heating rate for the case of oil-palm shell, but to increase for the case of oil-palm fibre and kernel. As to the order of reaction, when a higher heating rate is applied, the order of reaction tends to decrease for all materials.

4.4. Two-parallel reactions model

Fig. 8 compares the experimental data and model fitting using the two-parallel reaction model for the pyrolysis of oil-palm shell, fibre and kernel for various particle sizes and heating rates. Excellent agreement between the predicted results of the two-parallel reactions model and the experimental data is achieved under all pyrolysis conditions. Deviation of model prediction was found to be less than 4% for all samples and conditions (heating rate and particle size) being studied here. In addition, the two-parallel reaction model also shows an excellent description for the inflection of thermograms of oil-palm shell and fibre. Although, the two-step consecutive model of Guo and Lua (2001) can describe the experimental data of oil-palm shell and fibre quite well, its drawback is that the model consists of three ordinary differential equations which must be solved simultaneously. The accuracy of the model can be seriously affected by the size of time step and the numerical technique used. If smaller time step is applied, more accuracy can be obtained but more time is required for the computation. More importantly, as shown in the previous section the two-step consecutive model cannot account for the inflection of thermograms of oil-palm shell and fibre. On the other hand, the two-parallel reactions model proposed in the present work is more accurate and advantageous because it contains only one analytical solution, thus requiring much less computation time. However, it should be noted that the accuracy of the model calculation can be affected by the initial guess of the kinetic parameters used for the optimization step. Poor initial trials of the kinetic parameters may cause a large deviation in the model fitting.

Table 5 lists the kinetic parameters determined from the model simulation for oil-palm shell, fibre and kernel. The first fraction having higher activation energy could represent the decomposition of the heavier component (i.e. cellulose) which follows the first-order kinetic scheme. Larger values of b in comparison with the a values indicate that the pyrolysis of oil-palm shell and fibre are mainly contributed by the decomposition of the lighter components (i.e. hemicellulose) ($b = 79\%$ and 74% for palm shell and fibre, respectively). Tsamba et al. (2006) summarized the values of the activation energies of hemicellulose and

Table 4
Kinetic parameters of two-step consecutive model for pyrolysis of oil-palm shell, fibre and kernel

Sample	Heating rate (°C/min)	A_1 (s^{-1})	E_1 (kJ/mol)	A_2 (s^{-1})	E_2 (kJ/mol)	n	Max. error (%)
Shell	5	2.43×10^4	79.0	1.24×10^{25}	301.0	5.89	6.58
	10	6.99×10^4	82.1	3.89×10^{24}	299.3	5.24	4.37
	20	9.48×10^4	83.9	6.54×10^{23}	295.4	4.34	5.86
	40	3.65×10^5	86.3	2.80×10^{17}	221.8	2.94	5.04
Fibre	5	9.83×10^3	70.4	1.64×10^{29}	325.2	5.98	4.42
	10	9.73×10^3	71.4	7.93×10^{28}	326.3	5.69	3.80
	20	2.34×10^4	73.7	5.10×10^{28}	332.4	5.15	5.76
	40	4.92×10^4	74.5	4.55×10^{28}	339.8	4.90	5.19
Kernel	5	3.50×10^5	81.5	1.59×10^8	112.9	4.02	2.46
	10	6.78×10^5	82.5	2.43×10^9	174.2	3.62	2.82
	20	3.68×10^6	87.2	1.31×10^{10}	198.2	3.47	2.46
	40	8.19×10^6	87.6	1.89×10^{11}	136.7	2.56	4.33

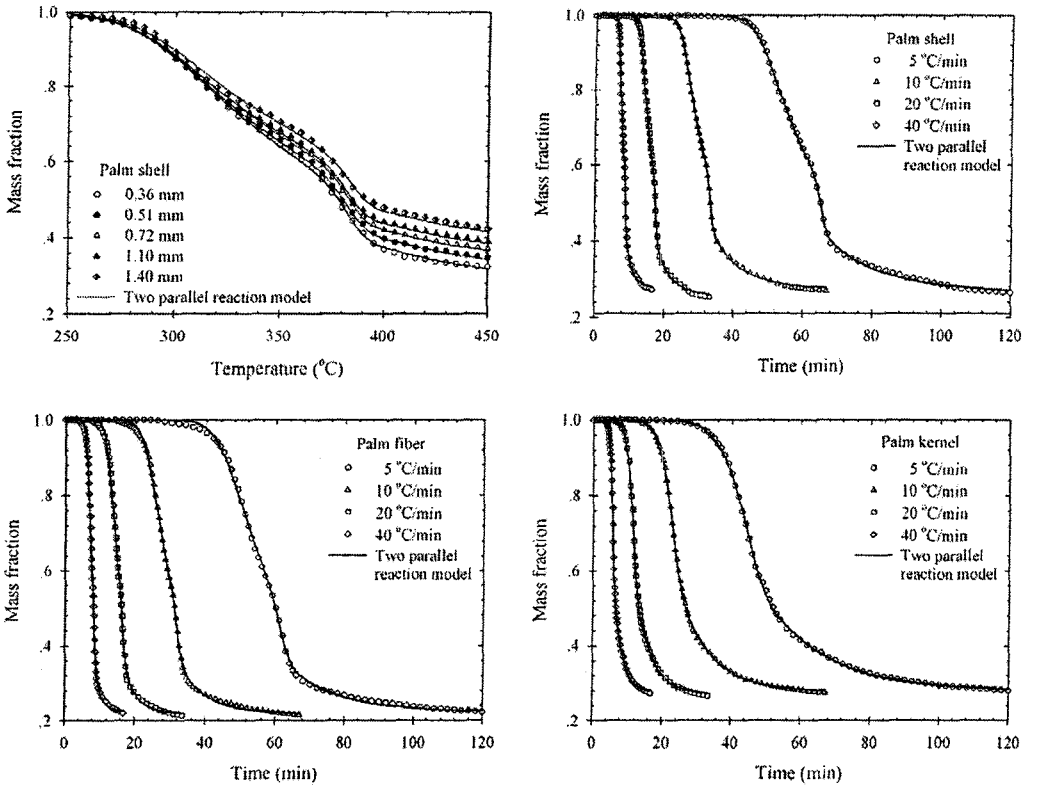

Fig. 8. TG data and two-parallel reaction model fitting for oil-palm shell, fibre and kernel pyrolyzed at different heating rate and particle sizes.

Table 5
Kinetic parameters (a, A_1, E_1, A_2, E_2 and n) of the two-parallel reactions model for pyrolysis of oil-palm shell, fibre and kernel

Sample	Heating rate (°C/min)	Size (mm)	a	A_1 (s^{-1})	E_1 (kJ/mol)	b	A_2 (s^{-1})	E_2 (kJ/mol)	n	Max. error (%)
Shell	5	0.36	0.21	9.82×10^{17}	243.1	0.79	1.15×10^{14}	173.2	4.02	2.81
	10			4.05×10^{16}	226.4		1.20×10^{14}	173.5	3.88	2.74
	20			2.43×10^{17}	238.9		4.58×10^{13}	169.8	3.50	2.61
	40			1.53×10^{17}	234.6		1.27×10^{14}	173.6	3.39	2.13
Shell	20	0.36	0.21	2.43×10^{17}	238.9	0.79	4.60×10^{13}	169.8	3.50	2.61
		0.51		7.48×10^{16}	232.8		8.61×10^{13}	172.2	3.67	2.60
		0.73		8.20×10^{16}	233.9		7.63×10^{13}	171.5	3.75	2.59
		1.10		1.08×10^{17}	234.4		6.56×10^{13}	170.1	3.95	2.98
		1.40		1.10×10^{17}	234.4		8.66×10^{13}	171.8	4.14	3.11
Fibre	5	<1.00	0.26	3.89×10^{16}	219.7	0.74	4.65×10^{14}	170.9	4.05	2.40
	10			9.04×10^{14}	201.8		1.86×10^{13}	156.8	3.69	2.71
	20			3.85×10^{15}	209.4		2.92×10^{12}	149.3	3.28	2.76
	40			2.57×10^{14}	193.7		3.21×10^{13}	158.2	3.38	2.64
Kernel	5	<0.15	0.60	2.44×10^{5}	80.0	0.40	4.29×10^{2}	54.8	2.37	2.28
	10			7.66×10^{5}	83.0		6.20×10^{2}	54.7	2.29	2.30
	20			3.58×10^{6}	87.4		2.07×10^{2}	47.9	2.04	2.66
	40			1.76×10^{7}	91.0		4.83×10^{2}	48.7	2.07	2.81

cellulose reported by previous studies. They found that the activation energy of hemicellulose is in the range of 147.24–172.75 kJ/mol and cellulose is in the range of 176.92–248.64 kJ/mol. For oil-palm shell and fibre, the fitted activation energy of the first fraction (E_1) agrees with that of cellulose and the fitted activation energy of the second fraction (E_2) agree with that of hemicellulose. These agreements further confirm that the first and second fractions could represent the decomposition of cellulose and hemicellulose, respectively. The variation of the kinetic parameters, including frequency factor, activation energy and reaction order for different heating rates and particle sizes can be further examined. It is noted that there is no definite trend for the frequency factor and activation energy when

the heating rate and particle size are changed. However, the reaction order of the second fraction (n) decreases with the increasing of heating rate but increases as the particle size is increased. Due to model simplification, the two-parallel reaction model assumes that the pyrolysis reaction is purely kinetic control where the effect of heat and mass transfer resistance are neglected. In principle, if the pyrolysis reaction is a true purely kinetic control, the kinetic parameters should be the same independent of heating rate and particle size. The observed variation of kinetic parameters as reported here may result from the complex scheme of pyrolysis reaction and also the effect of heat and mass transfer resistance existing in the real system.

In order to further confirm the validity of the two-parallel reactions model proposed in this study, we also applied this model to the data of other carbonaceous biomass materials, including coconut shell, bagasse, longan fruit seed and cassava pulp residue. All samples were pyrolyzed at 10 °C/min. The particle sizes of the samples are 0.36 mm for coconut shell, 0.1 mm for bagasse, 1.0 mm for longan seed and 0.23 mm for cassava pulp residue. Fig. 9 shows the experimental TG data and the simulated results which demonstrate that the two-parallel reactions model not only can describe well the pyrolysis of oil-palm solid wastes but it is also capable of predicting the pyrolysis behaviour of many other biomass materials. The maximum deviations for all materials are in the range of 1–4%. The kinetic parameters determined from the model fitting are listed in Table 6. The larger value of b in comparison with that of a indicates that the decomposition of coconut shell and bagasse are mainly contributed by the lighter fraction (second fraction). The thermograms of coconut shell and bagasse show the existence of inflection which is the same as in the case of the oil-palm shell and fibre. Based purely on these results, it is expected that the chemical compositions of coconut shell and bagasse are probably similar to

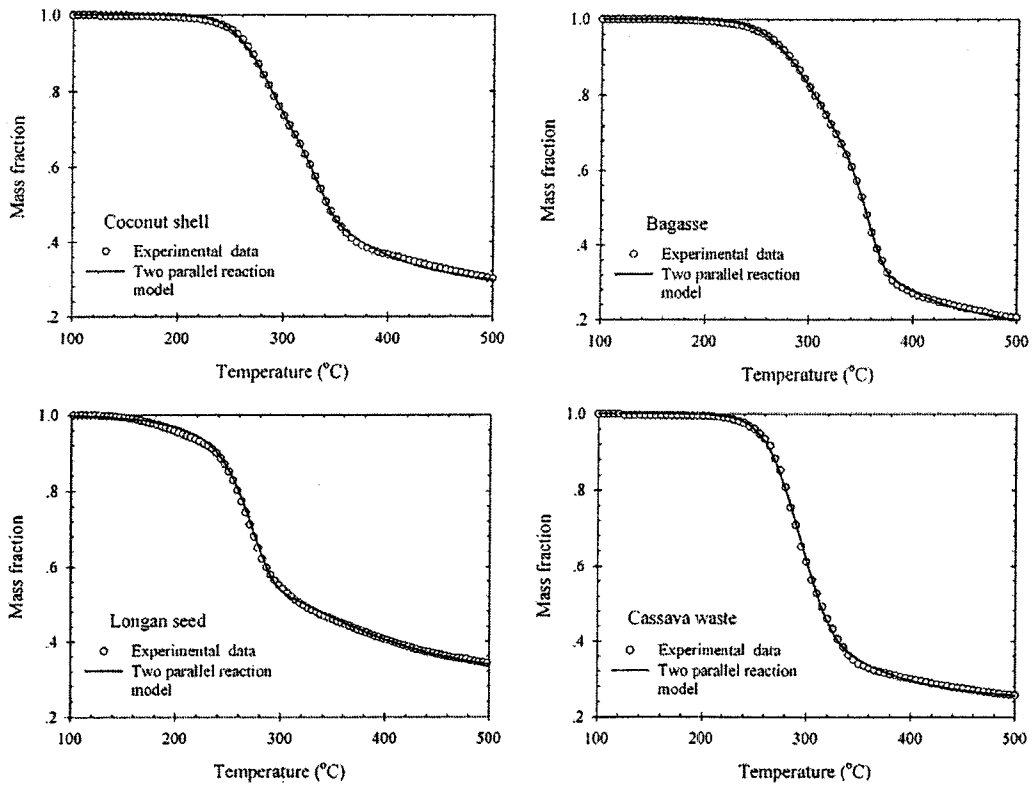

Fig. 9. TG data and model fitting for coconut shell, bagasse, longan fruit seed, cassava pulp residue pyrolyzed at 10 °C/min.

Table 6
Kinetic parameters of two-parallel reactions model for pyrolysis of coconut shell, bagasse, Longan seed, cassava pulp residue pyrolyzed at 10 °C/min

Sample	a	A_1 (s^{-1})	E_1 (kJ/mol)	b	A_2 (s^{-1})	E_2 (kJ/mol)	n	Max. error (%)
Coconut shell	0.14	4.26×10^{21}	254.20	0.86	9.74×10^{10}	138.77	3.43	3.53
Bagasse	0.30	2.68×10^{17}	233.76	0.70	4.54×10^{7}	106.26	3.35	3.16
Longan seed	0.47	1.23×10^{10}	126.96	0.53	1.20×10^{1}	30.55	1.41	1.41
Cassava pulp residue	0.49	7.66×10^{7}	110.0	0.51	7.22×10^{15}	218.2	3.13	3.15

those of the oil-palm shell and fibre. For longan seed and cassava pulp residue, the thermograms have no inflection of curve as exhibited also by the oil-palm kernel. The kinetic parameters show that the pyrolysis reactions of longan seed and cassava pulp residue are contributed equally by the first and second fractions (the values of a and b are comparatively the same). Similar conclusion can be inferred that the chemical compositions of these two materials are probably similar to that of the oil-palm kernel.

5. Conclusions

The non-isothermal thermogravimetric analysis of oil-palm solid wastes, including oil-palm shell, fibre and kernel shows significant influence of raw material size and heating rate on their pyrolysis behaviour. The pyrolysis process of oil-palm shell and fibre consist of two distinct kinetic schemes, while only one-step of kinetic scheme is observed for oil-palm kernel. The one-step global model is able to describe the thermal decomposition of oil-palm kernel, while the pyrolysis processes of oil-palm shell and fibre are best described by the two independent kinetic processes namely two-parallel reactions model proposed in this work. This model is capable of describing the experimental data with the maximum deviation being in the range of 2–4%. Since the two-parallel reaction model consists of 6 kinetic parameters, it is rather difficult to assign correct initial guesses of the kinetic parameters for the model optimization. As a result of this difficulty, some parameter should be determined experimentally, such as the initial fraction (a and b) of the first and second components.

Acknowledgement

Support of Royal Golden Jubilee Ph.D. program from The Thailand Research Fund (TRF) is gratefully acknowledged.

References

Antal, M.J., 1983. Biomass pyrolysis: a review of the literature. Part 1. Carbohydrate pyrolysis. In: Boer, K.W., Duffie, J.A. (Eds.), Advances in Solar Energy. American Solar Energy Society, Boulder, CO, pp. 61–111.

Bansal, R.C., Donnet, J.B., Stoeckli, F., 1988. Active Carbon. Marcel Dekker, New York.

Bellais, M., Davidsson, K.O., Liliedahl, T., Sjostrom, K., Pettersson, J.B.C., 2003. Pyrolysis of large wood particles: a study of shrinkage importance in simulations. Fuel 82, 1541–1548.

Caballero, J.A., Conesa, J.A., Font, R., Marcilla, A., 1997. Pyrolysis kinetics of almond shells and olive stones considering their organic fractions. Journal of Analytical and Applied Pyrolysis 42, 159–175.

Centre of Agricultural Information, 2004. Oil palm: harvested area, production and yield of major countries, Thailand.

Chan, W.R., Kelbon, M., Krigger, B.B., 1985. Product formation in the pyrolysis of large wood particles. In: Overend, R.P., Milne, T., Mudge, L. (Eds.), Fundamentals of Thermochemical Biomass Conversion. Elsevier Applied Science, New York, pp. 219–236.

Fisher, T., Hajaligol, M., Waymack, B., Diane, K., 2002. Pyrolysis behaviour and kinetics of biomass derived materials. Journal of Analytical and Applied Pyrolysis 62, 331–349.

Font, R., Marcilla, A., Verdu, E., Devesa, J., 1991. Thermogravimetric kinetic study of the pyrolysis of almond shells impregnated with $CoCl_2$. Journal of Analytical and Applied Pyrolysis 21, 249–264.

Guo, J., Lua, AC., 2001. Kinetic study on pyrolysis process of oil-palm solid waste using two-step consecutive reaction model. Biomass and Bioenergy 20, 223–233.

Haines, P.J., 1995. Thermal Methods of Analysis: Principles, Applications and Problems. Blackie Academic & Professional, UK.

Hartley, C.W.S., 1988. The Oil Palm, third ed. Longman Scientific & technical, New York.

Haykiri-Acma, H., 2006. The role of particle size in the non-isothermal pyrolysis of Hazelnut shell. Journal of Analytical and Applied Pyrolysis 75, 211–216.

Jayaweera, S.A.A., Moss, J.H., Thwaites, M.W., 1989. The effect of particle size on the combustion of weardale coal. Thermochimica Acta 152, 215–225.

Kok, M.V., Ozbas, E., Karacan, O., Hicyilmaz, 1998. Effect of particle size on coal pyrolysis. Journal of Analytical and Applied Pyrolysis 45, 103–110.

Larsen, M.B., Schultz, L., Glarborg, P., Skaarup-Jensen, L., Dam-Johansen, K., Frandsen, F., Henriksen, U., 2006. Devolatilization characteristics of large particles of tyre rubber under combustion conditions. Fuel 85, 1335–1345.

Pansamut, V., Pongrit, V., Intarangsi, C., 2003. The oil palm. Department of Alternative Energy Development and Efficiency. Ministry of Energy, Thailand.

Thurner, F., Mann, U., 1981. Kinetic investigation of wood pyrolysis. Industrial & Engineering Chemistry Process Design and Development 20, 482–488.

Tsamba, A.J., Yang, W., Blasiak, W., 2006. Pyrolysis characteristics and global kinetic of coconut and cashew nut shells. Fuel Processing Technology 87, 523–530.

Vamvuka, D., Kakaras, E., Kastanaki, E., Grammelis, P., 2003. Pyrolysis characteristics of biomass residuals mixture with lignite. Fuel 82, 1949–1960.

Wichman, I.S., Atreya, A., 1987. A simplified model for pyrolysis of charring materials. Combustion and Flame 68, 231–247.

Yaman, S., 2004. Pyrolysis of biomass to produce fuels and chemical feedstocks. Energy conversion and Management 45, 651–671.